Received: 4 July 2016 | Revised: 9 September 2016 | Accepted: 12 September 2016

DOI 10.1002/ppap.201600126

PLASMA PROCESSES AND POLYMERS

PLASMA PROCESSES AND POLYMERS

Full Paper

Waldo Bongers | Henny Bouwmeester | Bram Wolf | Floran Peeters | Stefan Welzel | Dirk van den Bekerom | Niek den Harder | Adelbert Goede | Martijn Graswinckel | Pieter Willem Groen | Jochen Kopecki | Martina Leins | Gerard van Rooij | Andreas Schulz | Matthias Walker | Richard van de Sanden

XX■Please provide a text together with a figure for the Graphical Table of Contents.■XX.

Journal	MSP No.	Dispatch: September 20, 2016	CE:
PPAP	201600126	No. of Pages: 8	PE: Katja Kornmacher

Received: 4 July 2016 | Revised: 9 September 2016 | Accepted: 12 September 2016

DOI 10.1002/ppap.201600126

PLASMA PROCESSES AND POLYMERS

FULL PAPER

Plasma-driven dissociation of CO_2 for fuel synthesis

Waldo[Q1] Bongers[1]* | Henny Bouwmeester[2] | Bram Wolf[1] | Floran Peeters[1] | Stefan Welzel[1] | Dirk van den Bekerom[1] | Niek den Harder[1] | Adelbert Goede[1] | Martijn Graswinckel[1] | Pieter Willem Groen[1] | Jochen Kopecki[3] | Martina Leins[4] | Gerard van Rooij[1] | Andreas Schulz[4] | Matthias Walker[4] | Richard van de Sanden[1,5]

[1] Dutch Institute for■**Affiliation link was not provide for the author Martijn Graswinckel, however, it has been linked with affiliation 1. Please check and if necessary.**■ Fundamental Energy Research (DIFFER), Eindhoven, The Netherlands

[2] MESA+ Institute for ■**Affiliations have been renumbered, please check.**■Nanotechnology, Inorganic Membranes, University of Twente, Enschede, The Netherlands

[3] Institute of Interfacial Process Engineering and Plasma Technology (IGVP), Universität Stuttgart, Stuttgart, Germany

[4] PHILIPS Technologie GMBH U-L-M Photonics, Ulm, Germany

[5] Plasma and Materials Processing Group, Department of Applied Physics, Eindhoven University of Technology, Eindhoven, The Netherlands

***Correspondence**
Waldo Bongers, Dutch Institute for Fundamental Energy Research (DIFFER), De Zaale 20, 5612 AJ Eindhoven, The Netherlands.
Email: w.a.bongers@differ.nl

Funding information
NWO■**Please check the presentation of grant sponsors for correctness.**■; FOM; RVO

Power-to-gas is a storage technology aiming to convert surplus electricity from renewable energy sources like wind and solar power into gaseous fuels compatible with the current network infrastructure. Results of CO_2 dissociation in a vortex-stabilized microwave plasma reactor are presented. The microwave field, residence time, quenching, and vortex configuration were varied to investigate their influence on energy- and conversion efficiency of CO_2 dissociation. Significant deterioration of the energy efficiency is observed at forward vortex plasmas upon increasing pressure in the range of 100 mbar towards atmospheric pressure, which is mitigated by using a reverse vortex flow configuration of the plasma reactor. Data from optical emission shows that under all conditions covered by[Q2] the experiments the gas temperature is in excess of 4000 K, suggesting a predominant thermal dissociation. Different strategies are proposed to enhance energy and conversion efficiencies of plasma-driven dissociation of CO_2.

KEYWORDS
CO_2-dissociation, efficiency, plasma, power-to-gas, solid-oxide-electrolyser

1 | INTRODUCTION

Sustainable energy sources will form a significant part of the global energy mix in 2025.[1] The intermittency and regional spread of renewable energy sources require efficient and large-scale storage and transport of energy in the form of synthetic chemical fuels, compatible to the present infrastructure. Such a Power-to-Gas (P2G) technology is based on electrically driven dissociation of CO_2 and H_2O to produce synthetic fuels such as syngas or methane. Methane can be formed either by direct internal reforming or via Fischer–Tropsch or Sabatier synthesis routes. Among the dissociation technologies of feedstock CO_2 and H_2O, solid oxide electrolysis and plasmolysis are considered as the most promising technologies.[1] Plasmolysis offers significant advantages over competitive technologies in that it can quickly adapt to a fluctuating supply of renewable sources, no scarce materials are employed, and overall energy efficiency is high, whilst

operation is in principle possible near ambient temperature and pressure.[2] In this paper, dissociation of CO_2 is studied using plasmolysis setups at DIFFER (Eindhoven, The Netherlands) and IGVP (Stuttgart, Germany).[3] The focus of the experiments is on optimization of the energy efficiency.

2 | PLASMA DISSOCIATION OF CO_2

The electron-induced dissociation of CO_2 is characterized by a high reaction enthalpy.[2]

$$CO_2 \rightarrow CO + O \qquad \Delta H = 5.5\,\text{eV}. \tag{1}$$

The formed atomic oxygen is able to react with another CO_2 molecule, according to reaction

$$CO_2 + O \rightarrow CO + O_2 \qquad \Delta H = 0.3\,\text{eV}. \tag{2}$$

The overall reaction can thus be represented by

$$CO_2 \rightarrow CO + \frac{1}{2}O_2 \qquad \Delta H = 2.9\,\text{eV}. \tag{3}$$

Dissociation of CO_2 in the plasma can take place via two possible mechanisms. The first is by thermal dissociation, which relies on a reversible shift in the chemical equilibrium towards the products induced by thermal heating. The dissociation fraction is governed by the gas temperature T_g and becomes significant at temperatures typically above 2000 K. Retention of the dissociation products is only achieved by a fast non-equilibrium cooling trajectory to prevent the reverse reaction. At a temperature of 3000 K, an optimal energy efficiency of 50% can be achieved under ideal quenching conditions.[4] This, however, does not take into account the possibility of heat recirculation, which can potentially lead to a higher overall energy efficiency. The quenching performance is determined by the instantaneous gas cooling rate, which is optimal between 10^7 and 10^9 K s^{-1} for full preservation of reaction species.[5] A super-ideal quenching mode has also been described.[2] Here, radicals and other short-lived activated species contribute to additional conversion in the quenching phase, leading to energy efficiencies up to 60%.[2]

The second mechanism of dissociation is initiated via electron-induced vibrational excitation. The vibrational dissociation is driven by non-equilibrium plasma conditions, which are characterized by a high vibrational temperature T_{vib}, and a low translational or gas temperature T_g of the CO_2 molecules. In the non-equilibrium regime, the plasma energy is efficiently deposited in the vibrational dissociation channel, while gas heating via other excitation channels of the CO_2 molecule is minimized. High efficiencies up to 90% have been reported,[6] but have not been reproduced until now.

The energy efficiency η of CO_2 dissociation is

$$\eta = \alpha \cdot \Delta H / SEI \tag{4}$$

where α is the fractional CO_2 conversion, defined as the ratio of the loss of CO_2 by dissociation to its feed into the reactor, ΔH the dissociation enthalpy for a CO_2 molecule (2.9 eV/molecule) and SEI the specific energy input (eV/molecule). Three main factors contribute to η[2]

$$\eta = \eta_{ex} \cdot \eta_{rel} \cdot \eta_{chem}. \tag{5}$$

The excitation factor η_{ex} is the fraction of discharge energy directed toward the relevant excitation channel. The coupling of electron energy to the asymmetric vibrational modes of CO_2 can be as high as 95% for an optimal electron energy distribution function (EEDF), which is achieved upon applying a reduced electric field (E/n) in a narrow range of typically 20–50 Td.[2,7]

The relaxation factor η_{rel} indicates the extent in which the principle active species are conserved for the reaction rather than being quenched via, for example, relaxation or recombination. Vibrational relaxation is primarily determined by the vibrational-to-translational (VT) relaxation process, which has a strong positive dependence on T_g.[2,8] Specifically at moderate to low T_g and large values of η_{ex}, a strong VT decoupling ($T_{vib}/T_g > 30$) occurs and a VT non-equilibrium plasma can be sustained.[6] Additionally, the particle residence time in the plasma in relation to the characteristic VT relaxation time is found to play an important role in determining the value of η_{rel}.[7] It is reasoned that as long as the characteristic excitation time – approximated by the particle residence time – is much shorter than the characteristic relaxation time, the active (vibrational) species should be well conserved.

Lastly, the chemical factor η_{chem} indicates the efficiency of the principle active discharge species in driving the

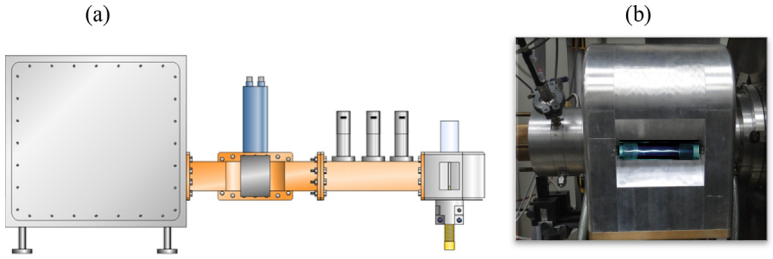

FIGURE 1 (a) Schematics of the 915 MHz 3–30 kW plasma setup at IGVP. The system is equipped with (from left to right) a magnetron, circulator, straight waveguide, 3-stub tuner (all WR-975), and the plasma source, consisting of a quartz tube placed inside the TM_{010} cylinder mode cavity with tangential gas injection. (b) Photograph of the plasma source

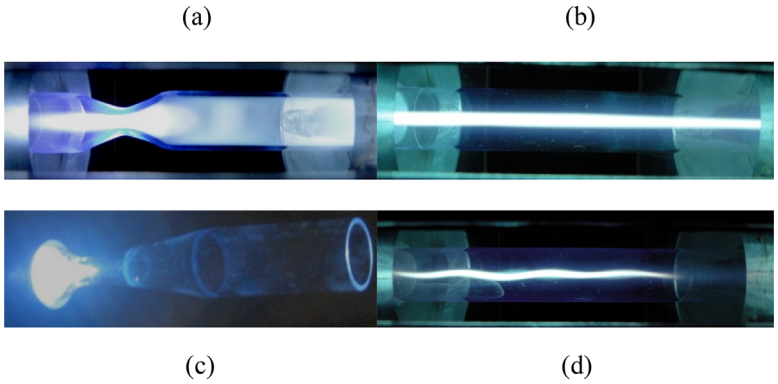

FIGURE 2 Photographs of the plasma obtained using the 915 MHz plasma reactor: (a) supersonic expansion of the plasma in the MW cavity at 1 mbar gas pressure; (b) plasma in the MW cavity (MW power 5.0 kW; flow rate 11 slm; pressure 200 mbar); (c) subsequent quenching of the plasma after the nozzle into the vacuum vessel (1 mbar), and (d) plasma in the MW cavity (MW power 3.1 kW; flow rate 75 slm; pressure 200 mbar). Note the supersonic shockwaves after the nozzle in (a)

chemical reaction of interest. In general, any surplus of the vibrational energy above the reaction enthalpy involved in the dissociation process is lost and decreases the η_{chem}. Vibrational CO_2 dissociation is relatively efficient since the process involves a so-called "ladder-climbing" process with small vibrational quanta, in contrast to for instance electron-impact excitation dissociation, where a large surplus of electron energy from the tail of the EEDF can be converted to heat.[9] An additional contribution that limits η_{chem} relates to the oxygen radical chemistry.[7] Depending on the pressure, the atomic oxygen produced in reaction (1) may recombine at the wall to form O_2 or take part in reaction (2). Only in the latter case, an average minimum energy for dissociation of CO_2 of ~2.9 eV/molecule is required. The rates of reactions (1) and (2) should be similar to meet this requirement.

In summary, E/n, T_g, residence time and the oxygen radical chemistry are important parameters for optimisation of the vibrational dissociation of CO_2. High vibrational activation and low VT relaxation can be achieved by applying a narrow range of E/n, keeping a low value of T_g, and using a short residence time in comparison to the characteristic VT-relaxation time.

3 | EXPERIMENTAL SECTION

In this study, the influence of microwave (MW) field, residence time in the plasma reactor, quenching, and vortex plasma configurations on energy efficiency of CO_2 dissociation was investigated. Plasma experiments were carried with two different setups. At IGVP, the experiments were conducted using a 915 MHz plasma system using WR-975 waveguide components with dimensions 24.8×12.4 mm^2. The plasma source of this system is based on a transverse magnetic cylinder mode cavity (TM_{010}, with internal diameter of 225 mm) through which a quartz tube (with internal/external diameter of 30 mm/34 mm) is inserted.[10] The schematics and a photograph of the plasma source are shown in Figure 1. At DIFFER, a 2.45 GHz 1 kW plasma system (InitSF) with WR-340 waveguide components with dimensions 86.4×43.2 mm^2 was used. Distinct from the setup shown in Figure 1, a quartz tube (with internal/external diameter of 27 mm/30 mm) was placed inside the transverse electric rectangular waveguide cavity to form a TE_{101} mode. To enhance the field at the gas injection location, a central resonator pin was used to form a circular transverse electromagnetic mode coaxial cavity coupled to the rectangular waveguide mode cavity. The 3-stub tuner was used to minimize the reflected power and to

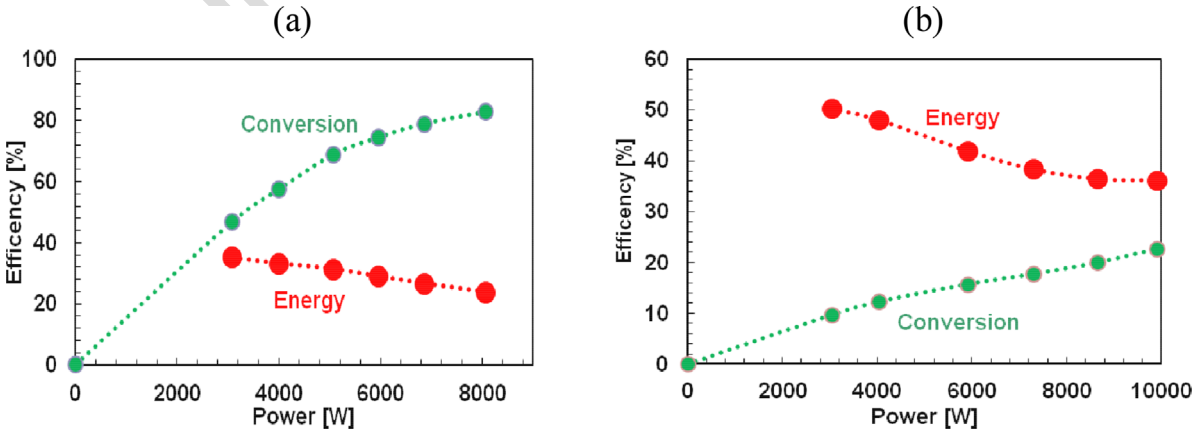

FIGURE 3 Energy and conversion efficiencies in quenching experiments, using the 915 MHz plasma reactor. Data were obtained at a CO_2 gas flow rate of (a) 11 slm, and (b) 75 slm, both at a plasma pressure of 200 mbar

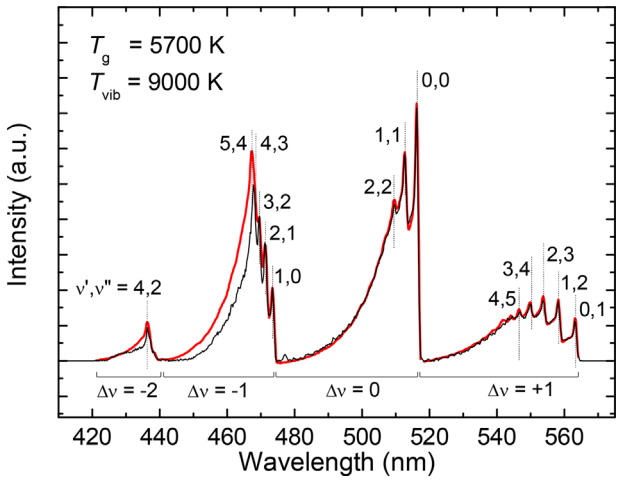

FIGURE 4 Experimental (black) and simulated (red) C_2 (d $^3\Pi_g \rightarrow$ a $^3\Pi_u$) Swan bands. Experimental data were obtained at 0.9 eV/molecule (MW power 5 kW; CO_2 gas flow rate 75 slm) and at a plasma pressure of 200 mbar. The measured spectrum is baseline-corrected, that is, contributions from broadband continuum radiation were subtracted. The C_2 (d $^3\Pi_g$, v′ → a $^3\Pi_u$, v″) transitions are indicated

measure the actual plasma impedance. The MW electrical field was calculated from the plasma impedance using the ANSYS HFSS electromagnetic software package.[11]

The vortex in both setups was created by tangential gas injection nozzles. In case of 915 MHz plasma source, a single nozzle (4 mm internal diameter) was used, whereas a double nozzle (1 mm internal diameter) was used for the 2.45 GHz InitSF plasma system. The product formation in both setups was measured downstream using a mass spectrometer (MS) (Hiden HAL RC 201QIC with a capillary inlet) relative to calibrated reference gas mixtures. Optical emission spectroscopy (OES) (HR2000 and HR4000, Ocean Optics) was used to identify the constituents of the plasma and to determine their rotational temperature T_{rot} and vibrational temperature T_{vib}. Spectra were collected via an optical fibre pointing at the brightest point of the plasma in the centre of the quartz tube. A relative calibration was carried out to correct for variations in fibre transmittance and spectrometer sensitivity as a function of wavelength. Simulation of the C_2 Swan bands and emission intensities for electronic transitions in emitting diatomic molecules was carried out using SpecAir,[12] which enabled evaluation of the T_{rot} and T_{vib} of the C_2 molecules, which are assumed to be in thermal equilibrium with heavier molecular species in the plasma. The shape of C_2 Swan bands is determined only by these temperatures, and is independent of the absolute intensity of the emission so that a relative calibration of the experimental spectra suffices.

4 | RESULTS AND DISCUSSION

4.1 | CO_2 dissociation experiments using the 915 MHz MW reactor at IGVP

Several forward vortex (FV) plasma configurations were investigated using the 915 MHz reactor at IGVP with a MW power up to 10 kW.[2] In supersonic plasma expansion experiments, a constriction (nozzle) in the quartz tube expanded the plasma into the cavity.[13] The experiments were conducted at ~1 mbar gas pressure. In quenching experiments, in which the gas pressure was ~200 mbar, the nozzle was positioned after the cavity, such that the exhaust gas expanded supersonically. The latter configuration was intended to quench the plasma gas and to freeze the conditions of CO_2 dissociation. Figure 2 presents photographs of the obtained plasmas in both configurations.

The supersonic expansion experiments using the 915 MHz MW plasma reactor showed a maximum η of 15% in the range of MW power 3–10 kW. Following Fridman,[2] such a low value of η can be explained by a low plasma pressure. Both energy and conversion efficiencies were found to be much higher in quenching experiments as described below.

In quenching experiments, the energy and conversion efficiencies varied from $\eta = 24\%$ and $\alpha = 83\%$ at a *SEI* of 10.3 eV/molecule (MW power 8.1 kW) to $\eta = 35\%$ and $\alpha = 47\%$ at a *SEI* of 3.9 eV/molecule (MW power 3.1 kW), as

TABLE 1 Operating conditions and configurations maintained during different experiments using the 2.45 GHz plasma source (InitSF) at DIFFER■**Please check the presentation of table note for correctness.**■

Experiment	Configuration	Flow-type	Field enhancement	Quenching	SEI [eV/molecule]
(1)	A	FV	No[a]	–	0.9
(2)	B	FV	Half-height WG	–	0.9
(3)	C	FV	No[a]	Conductive	0.9
(4)	C	FV	Resonator pin[a]	Conductive	0.9
(5)	C	RV	No[a]	Convective	0.9
(6)	A	FV	No[a]	–	1.7
(7)	C	RV	No[a]	Convective	0.8
(8)	C	RV	No[a]	Convective	1.7

Photographs of the different configurations are given in Figure 5.
[a]Full-height waveguide (WG) configuration.

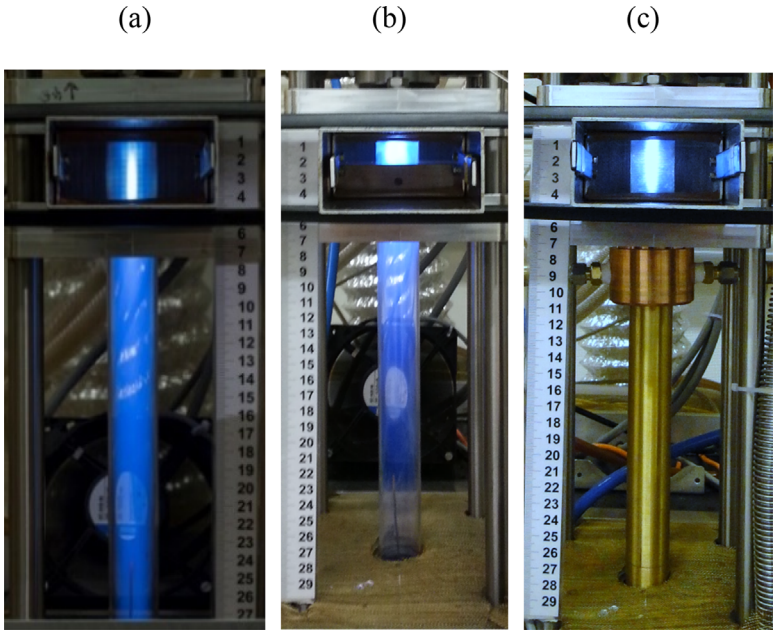

FIGURE 5 Different configurations of the 1 kW 2.45 GHz plasma source at DIFFER, denoted as (a) A, (b) B, and (c) C in Table 1. In all cases the plasma is seen through a metal grid, which acts as a short-circuit of the TE_{10} mode in the waveguide cavity. The CO_2 gas is tangentially injected from the top just above the waveguide cavity to create a vortex gas flow separating the visible part of the plasma from the quartz tube. Photographs were recorded using gas pressures (a) 130 mbar, (b) 150 mbar, and (c) 130 mbar

shown in Figure 3a. η and α increases and decreases, respectively, if the *SEI* is reduced, as expected from literature.[2] To lower the *SEI* range, the CO_2 gas flow rate was increased from 11 to 75 slm. Figure 3b confirms that η increased from 40 to 51%, and α decreased from 23 to 11%, upon decreasing the *SEI* from 1.9 eV/molecule (MW power 10 kW) to 0.6 eV/molecule (MW power 3.1 kW). A photograph of the plasma obtained at an input gas flow rate of 75 slm and a *SEI* of 0.6 eV/molecule (MW power 3.1 kW) is shown in Figure 2d. Below a MW power of 3.1 kW, the plasma could not be sustained.

Optical emission data of the C_2 (d $^3\Pi_g$, v′ → a $^3\Pi_u$, v″) Swan bands are shown in Figure 4. These data were obtained using the plasma configuration shown in Figure 2d. At the moderate pressures used in this work, the C_2 molecules are assumed to be in thermal equilibrium with heavier molecular species in the plasma. Hence, the shape of the Swan bands is determined by the values of T_{rot} and T_{vib} of these constituents.[14] The value of T_{rot} is assumed to be equal to the translational gas temperature T_g. The latter is supported by the good agreement between the simulated data of T_{rot} and those of T_g measured previously in our laboratory using Rayleigh scattering on MW plasmas created under conditions similar to those used in the present study.[4] The value of T_{vib} serves as an indicator for the VT non-equilibrium at given T_g. For the bands $\Delta\nu = 0$ and +1, the observed spectra match well with the simulated spectra for T_g = 5700 K and T_{vib} = 9000 K. For the bands with $\Delta\nu = -1$ and −2, the simulated spectra depart significantly from the measured ones. A similar departure was observed in a MW plasma study using CO_2–Ar mixtures by Spencer and Gallimore.[15,16] The discrepancy is attributed to the fact that only a single value of T_{vib} is used in simulation for the fitting. The clear difference between T_g and T_{vib} at $\nu' < 4$ points to a significant VT non-equilibrium in the plasma. Whether this holds for the vibrational distribution of all heavy species in the plasma is uncertain. Due to a high VT relaxation rate at T_g = 5700 K thermal dissociation of CO_2 is predominant at this temperature.[2,4,9]

4.2 | CO_2 dissociation experiments using the 2.45 GHz MW Reactor at DIFFER

Several experiments were performed using different reactor configurations (flow type, field enhancement, and quenching) of the 2.45 GHz plasma source (InitSF) at DIFFER. Experiments and configurations are listed in Table 1. Experiments (1) and (2) were conducted using the reactor in the FV flow configuration,[16] with the gas inlet before and the exhaust after the MW cavity, both at full- and half-height waveguide configurations, and at a *SEI* of 0.9 eV/molecule (MW power 1 kW; CO_2 gas flow rate 14 slm), in order to investigate the influence of electric field and residence time on η. Corresponding photographs of the plasmas obtained for both configurations, denoted as A and B in Table 1, are shown in Figure 5a and b, respectively. In Experiment (3), conductive quenching of the outlet gas was applied to prevent backward reactions. Quenching was achieved by placing a water-cooled brass quencher with a nozzle (~5 mm

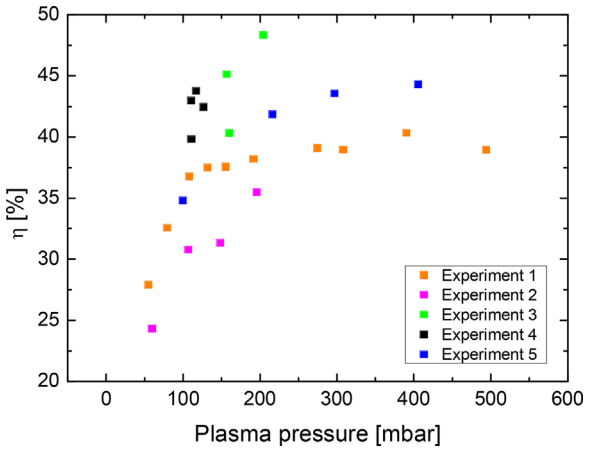

FIGURE 6 Energy efficiency η as a function of plasma pressure during different tests using the InitSF plasma reactor. Experimental conditions and configurations maintained during these tests are listed in Table 1. Standard errors (95% confidence interval of the mean) are within 3%

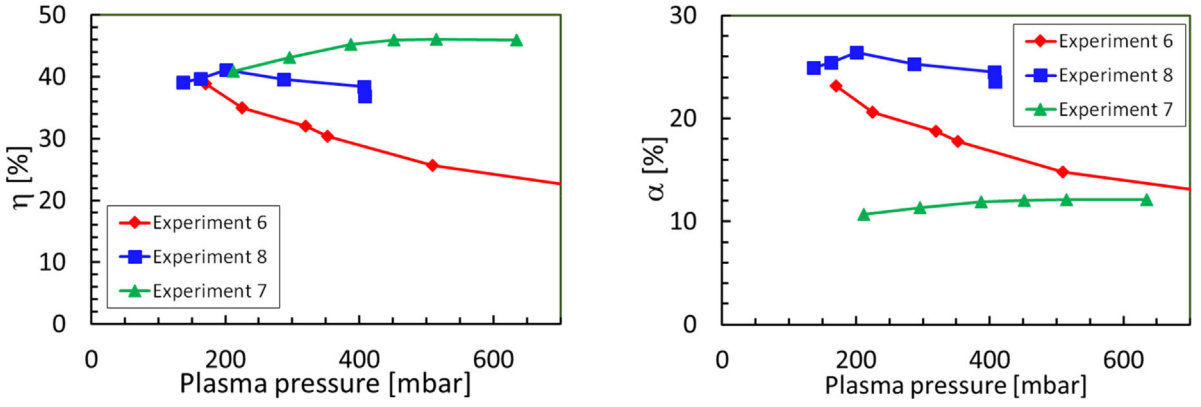

FIGURE 7 (a) Energy and (b) conversion ■**Figure subparts are not mentioned in art work, please check.**■efficiency as a function of plasma pressure obtained from measurements using the InitSF plasma reactor. Experimental conditions and configurations maintained during these tests are listed in Table 1. Standard errors (95% confidence interval of the mean) are within 3%

constriction) in the exhaust of the reactor operated at full-height waveguide. A photograph of the plasma obtained for this configuration, denoted as C in Table 1, is shown in Figure 5c. In Experiment (4), a resonator pin was installed inside the gas inlet system to enable transverse electromagnetic mode coaxial cavity at the gas inlet to increase the field at equal waveguide height. In Experiment (5), the InitSF plasma reactor was operated in the reverse vortex (RV) flow with the bottom exhaust/quencher closed in order to have both gas input (tangential) and output (central) at the top. A copper quenching tube as short as ~2 cm was placed inside the coaxial cavity to optimize heat exchange between input and output gas.

Values of η as a function of plasma pressure obtained during different tests recorded at a *SEI* of 0.9 eV/molecule are shown in Figure 6. In the basic FV configuration (Experiment (1)), that is, without additional quenching, η reaches up to ~40% at a plasma pressure of 400 mbar. *E/n* is in the range 70–80 Td for the reactor in the full-height waveguide configuration, corresponding to an average electron energy >2 eV.[18] According to Fridman,[2] a value for *E/n* of ~20 Td is required to obtain the appropriate electron energy distribution function (EEDF) for exciting the asymmetric vibrational mode of the CO_2 molecule. As can be seen from Figure 6, the value of η drops upon halving the height of the waveguide (Experiment (2)), that is, upon enhancing the electric field. In Experiment (3), having the reactor in the full-height waveguide configuration and with additional quenching, η increases to a maximum value of ~47% at a plasma pressure of 200 mbar. However, in this mode of operation the plasma could not be sustained at pressures higher than 200 mbar. In Experiment (4), the electric field within the plasma is enhanced by application of a resonator pin. As can be seen from Figure 6, η is found in the range 40–43% at gas pressures ~100 mbar. Quenching leads to unstable plasma operation in the FV configuration. Operating the reactor in the

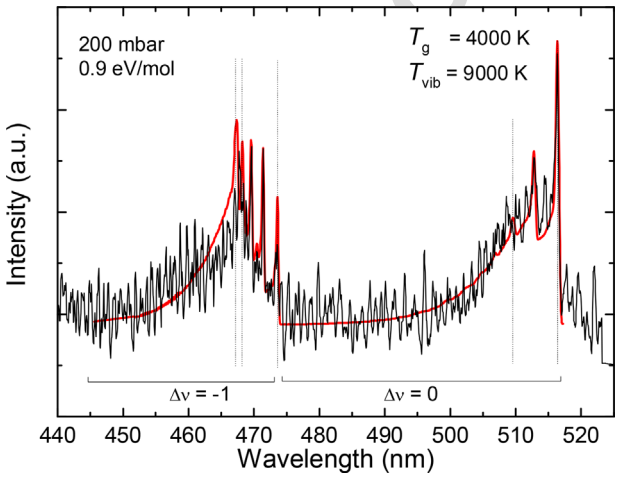

FIGURE 8 Measured (black) and simulated (red) $C_2(d\ ^3\Pi_g \rightarrow a\ ^3\Pi_u)$ Swan bands. Measured data were obtained at a *SEI* of 0.9 eV/molecule (MW power 1 kW; CO_2 gas flow rate 14 slm), and at a plasma pressure of 200 mbar. The measured spectrum is baseline-corrected, that is, contributions from broadband continuum radiation were subtracted

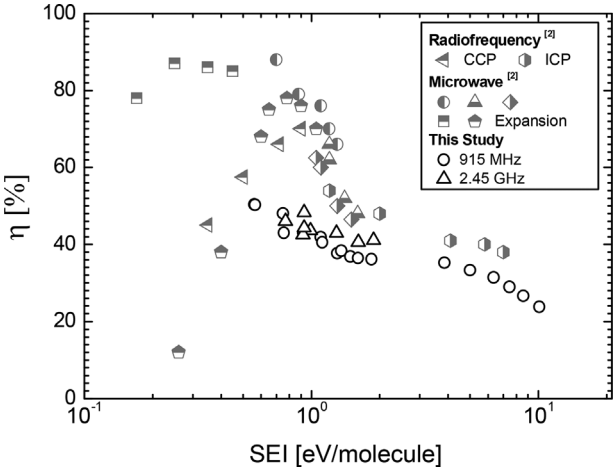

FIGURE 9 Energy efficiency η as a function of SEI. Comparison of results from this study with data reported by Fridman.[2] Results from Fridman are presented for radiofrequency (3–30 MHz) and microwave (915–2.45 GHz) discharges with and without expansions

RV flow configuration (Experiment (5)), shifts operation again to higher plasma pressures, achieving the highest value of $\eta = 46\%$ at 500 mbar.

Values of η and α as a function of plasma pressure from Experiments (6), (7), and (8) ■**See Table 1 are plotted in ... when using a FV flow (Experiment (6)). The meaning of this sentence is not clear; please rewrite or confirm that the sentence is correct.**■(see Table 1 are plotted in Figure 7a and b, respectively. The main purpose of these tests was to show the effect of flow pattern and *SEI* on both efficiencies with the reactor in FV and RV flow configurations. As seen from Figure 7, both η and α decrease with increasing plasma pressure when using a FV flow (Experiment (6)). The results further show that at similar value of *SEI* an improved performance is obtained when the reactor is configured to have a RV flow. This might be explained by two factors: firstly, the radial pressure gradient in the RV flow maintains more excited particles within the plasma volume compared to when using a FV flow, and secondly, the output gas in the RV flow configuration is quenched by the input gas.

The optical emission from $C_2(d\ ^3\Pi_g, \nu' \rightarrow a\ ^3\Pi_u, \nu'')$ Swan bands was measured during Experiment (1) in the core of the plasma. Corresponding data are shown in Figure 8. Simulation of the Swan bands gave $T_g = 4000$ K and $T_{vib} = 9000$ K at a *SEI* of 0.9 eV/molecule. The values again point to a significant VT non-equilibrium in the plasma. The high value of T_g indicates a minor contribution of vibrational excitation to the rate of CO_2 dissociation due to a high VT relaxation rate. The high T_g gives rise to a relatively high *E/n* since the plasma gas density drops with increasing temperature.

5 | CONCLUDING REMARKS

The experiments using the plasmolysis setups at IGVP and DIFFER, operating at 915 and 2.45 GHz, respectively, show that for plasma dissociation of CO_2 values of η as high as ~50% can be achieved. Figure 9 shows a comparison of η as a function of *SEI* from this study with corresponding survey of data reported by Fridman.[2] In general, lower values of η are obtained at higher *SEI* values. Clear discrepancies between the results from this study and those reported by Fridman occur below a *SEI* of 1 eV/molecule. Fridman's data are claimed to be characterized by a strong VT non-equilibrium in the plasma.[2]

The results from this study are obtained near the maximal thermal equilibrium dissociation limit, which indicates that the thermal dissociation mechanism is predominant. The latter is in agreement with the observations made by optical emission spectroscopy, which indicate that the values of T_g in the plasmas of both setups under chosen experimental conditions are too high to achieve VT non-equilibrium conditions. Similar observations have been reported previously.[4,9,19] Quenching of the plasma has a beneficial effect on η. In this study, quenching could enhance η to a maximum value of ~47% at a plasma pressure of 200 mbar. This observation is predicted by Fridman for plasmas in the thermal regime.[2]

A number of possible explanations for the observed thermal behavior of plasma dissociation of CO_2 can be given. The observed decrease of η upon enhancing the electrical field as well as the electromagnetic simulations of the cavity electric field distribution in the plasma indicate that values of 70–80 Td for *E/n* are too high, where values of 20–50 Td are optimal for high- temperature plasmas.[2,7] It should be noted that the value of T_g has a significant influence on *E/n* since the plasma density is inversely proportional to T_g. High temperatures in the plasmas core may account for the observed high values of *E/n*. Furthermore, the VT relaxation rate has a strong dependence on T_g. Hence, the temperature during discharge should be as low as possible to reduce vibrational energy losses via VT relaxation.[2,7] Future experiments will be directed towards reducing *E/n*, by increasing the cavity dimensions, and reduction of T_g by lowering the temperature of the injected gas.[20,21]

A known issue with plasma dissociation of CO_2 at high η is that there is an upper limit in the conversion.[2] Recently, researchers from the Tokyo Institute of Technology explored a hybrid reactor, integrating a dielectric barrier discharge (DBD) plasma reactor and a solid oxide electrolysis cells (SOEC's).[25] CO_2 conversion was significantly enhanced in the hybrid reactor. Complete CO_2 conversion was found at a temperature as low as 600 °C.[26] These results were obtained using a simple DBD, which is known to have a low η (< 5%). The value of η of a MW plasma reactor is known to be one order of magnitude higher.[2,6] It can be expected that the synergistic integration of high-temperature SOECs into a MW plasma reactor holds promise for dissociation of CO_2.

6 | LIST OF SYMBOLS AND ABBREVIATIONS ■PLEASE CHECK THE PLACEMENT AND PRESENTATION OF ABBREVIATIONS FOR CORRECTNESS.■

α	fractional CO_2 conversion/conversion efficiency (−)
ΔH	reaction enthalpy or dissociation enthalpy for a CO_2 molecule (eV)
η	energy efficiency (−)
η_{chem}	chemical factor (−)
η_{ex}	excitation factor (−)
η_{rel}	relaxation factor (−)
DBD	dielectric barrier discharge
E/n	reduced electrical field (Td)

EEDF	electron energy distribution function
FV	forward vortex
InitSF	Initial solar fuel plasma reactor at DIFFER
MS	mass spectrometer
MW	microwave
OES	optical emission spectroscopy
RV	reverse vortex
SEI	specific energy input (eV/molecule)
SOEC	solid oxide electrolysis cell
TEM	transverse electromagnetic
T_g	gas temperature (K)
T_{rot}	rotational temperature (K)
T_{vib}	vibrational temperature (K)
ν	vibrational quantum number
VT	vibrational-to-translational
WG	waveguide

ACKNOWLEDGMENTS

The authors acknowledge the support by NWO, FOM, and RVO within the Dutch framework of "Top sector energy" within the tender "System function of gas" of TKI gas. This work was partially carried out under RVO project (grant nr. TEG0413006) in collaboration with Alliander, Gasunie and Energy Valley.

REFERENCES

[1] C. Graves, S. D. Ebbesen, M. Mogensen, K. S. Lackner, *Renew. Sust. Energy Rev*. **2011**, *15*, 1.

[2] A. Fridman, *Plasma Chemistry*, Cambridge University Press, New York **2008**.

[3] A. P. H. Goede, W. A. Bongers, M. F. Graswinckel, M. Leins, J. Kopecki, A. Schulz, M. Walker, *EPJ Web Conf*. **2014**, *79*, 01005.

[4] N. den Harder, D. C. M. van den Bekerom, M. F. Graswinckel, J. M. Palomares, F. J. J. Peeters, S. Ponduri, T. Minea, W. A. Bongers, M. C. M. van de Sanden, G. J. van Rooij, *Plasma Process. Polym*. **2016**, this issue.■**Please provide volume number and page range for the references [4, 8, 10].**■

[5] L. Chiappetta, M. B. Colket, *J. Heat Transf*. **1984**, *106*, 460.

[6] V. D. Rusanov, A. Fridman, G. V. Sholin, *Usp. Fiz. Nauk*. **1981**, *134*, 185.

[7] T. Kozák, A. Bogaerts, *Plasma Sources Sci. Technol*. **2014**, *23*, 045004.

[8] J. A. Blauer, G. R. Nickerson, *Ultrasystems Inc. Tech. Report* **1973**.

[9] G. J. van Rooij, et al., *Faraday Discuss*. **2015**, *183*, 233–248. ■**Please provide the list of all the authors for references [9, 25].**■

[10] M. Leins, L. Alberts, M. Kaiser, M. Walker, A. Schulz, U. Schumacher, U. Stroth, *Plasma Process. Polym*. **2009**.

[11] Avilable at: http://www.ansys.com/Products/Electronics/ANSYS-HFSS.

[12] Avilable at: http://www.specair-radiation.net/.

[13] R. I. Azizov, A. K. Vakar, V. K. Zhivotov, M. F. Krotov, OA Zinov'ev, B. V. Potapkin, V. D. Rusanov, A. A. Rusanov, A. A. Fridman, *Sov. Phys. Dokl*. **1983**, *28*, 567.

[14] G. Lombardi, B. Benedic, F. Mohasseb, K. Hassouni, A. Gicquel, *Plasma Sources Sci. T*. **2004**, *13*, 375.

[15] L. Spencer, *The Study of CO_2 Conversion in a Microwace/Catalyst System, PhD Thesis*, University of Michigan, **2012**.■**Please provide publisher's place for the reference [15].**■

[16] L. Spencer, A. D. Gallimore, *Plasma Chem. Plasma P*. **2011**, *31.1*, 79.

[17] Yu. P. Butylkin, V. K. Givotov, E. G. Krasheninnikov, V. D. Rusanov, A. Fridman, *Sov. Phys. J. Tech. Phys*. **1981**, *51*, 925. ■**References [17, 22−24] have not beem listed in the text, please check.**■

[18] A. Fridman, L. A. Kennedy, *Plasma Physics and Engineering*, Taylor & Francis, New York, London **2004**.■**Please check the presentation of authors name for correctness.**■

[19] A. Essiptchouk, High pressure plasma reactor for thermal dissociation of carbon dioxide, *ESCAMPIG XX* **2012**.

[20] T. Verreycken, P.M.J. Koelman, D.C.M. van den Bekerom, J.M. Palomares-Linares, S. Ponduri, J. van Dijk, G.J. van Rooij, M.C.M. van de Sanden, W.A. Bongers, Investigation of the effect of on- and off time on the dissociation of CO_2 in a pulsed microwave discharge, *submitted to EPJ AP*, 15th *High pressure low temperature plasma chemistry symposium, September 11–16, Brno, Czech Republic* **2016**.

[21] N. A. Zyrichev, S. M. Kulish, V. D. Rusanov, *CO_2 Dissociation in Supersonic Plasma-Chemical Reactor*, Kurchatov Institute of Atomic Energy, Moscow **1984**, vol. *4045*, p. 6.

[22] A. K. Vakar, V. K. Givotov, E. G. Krasheninnikov, A. Fridman, *Sov. Phys. J. Techn. Phys. Lett*. **1981**, *7*, 996.

[23] T. Nunnally, K. Gutsol, A. Rabinovich, A. Fridman, A. Gutsol, A. Kemoun, *J. Phys. D: Appl. Phys*. **2011**, *44*, 274009.

[24] V. K. Givotov, E. G. Krasheninnikov, M. F. Krotov, V. D. Rusanov, A. Fridman, *3rd World Hydrogen Energy Conference, Tokyo* **1980**, 92.

[25] Y. Tagawa, et al., *Kagaku Kogak Ronbunshu* **2011**, *37*, 114.

[26] L. L. Tun, N. Matsuura, S. Mori, *22nd International Symposium on Plasma Chemistry*, **2015**, O-15-3.

AUTHOR QUERY FORM

JOURNAL: PLASMA PROCESSES AND POLYMERS

Article: ppap201600126

Dear Author,

During the copyediting of your paper, the following queries arose. Please respond to these by annotating your proofs with the necessary changes/additions using the E-annotation guidelines attached after the last page of this article.

We recommend that you provide additional clarification of answers to queries by entering your answers on the query sheet, in addition to the text mark-up.

Query No.	Query	Remark
Q1	Please confirm that given names (red) and surnames/family names (green) have been identified correctly.	
Q2	Please clarify throughout the article all editorial/technical requests marked by black boxes.	

Plasma Processes and Polymers

Editorial office:
Wiley-VCH
Plasma Processes and Polymers
Boschstrasse 12, 69469 Weinheim
Germany

Tel.: +49 (0) 6201 606 – 581 or 238
Fax: +49 (0) 6201 606 – 510
E-mail: plasma@wiley-vch.de

Reprint Order Form 2015

Short DOI: ppap._____

Please send me and bill me for

☐ no. of **Reprints** via ☐ airmail (+ 25 Euro) ☐ surface mail

Please send me and bill me for a

☐ **high-resolution PDF file** (330 Euro).

My e-mail address:

_____

Please note: It is not permitted to present the PDF file on the internet or on company homepages

Information regarding VAT
Please note that from German sales tax point of view, the charge for **Reprints, Issues or Posters** is considered as **"supply of goods"** and therefore, in general, such delivery is a subject to German sales tax. However, this regulation has no impact on customers located outside of the European Union. Deliveries to customers outside the Community are automatically tax-exempt. Deliveries within the Community to institutional customers outside of Germany are exempted from the German tax (VAT) only if the customer provides the supplier with his/her VAT number. The VAT number (value added tax identification number) is a tax registration number used in the countries of the European Union to identify corporate entities doing business there. It starts with a country code (e.g. FR for France, GB for Great Britain) and follows by numbers.

Mail reprints / posters to:

_____
_____
_____
_____
_____

Invoice address:

_____
_____
_____
_____
_____

VAT no.: _____
(Institutes / companies in EU countries only)

Purchase Order No.: _____

Credit Card Payment:

VISA, MasterCard, AMERICAN EXPRESS
Please use the Credit Card Token Generator located at the website below to create a token for secure payment. The token will be used instead of your credit card number.

Credit Card Token Generator:
https://www.wiley-vch.de/editorial_production/index.php

Please transfer your token number to the space below.

Credit Card Token Number

Cover Posters

Posters are available of all the published covers and frontispieces in two sizes

☐ DinA2 42 x 60 cm/ 17 x 24in (one copy: **39 Euro**)

☐ DinA1 60 x 84 cm/ 24 x 33in (one copy: **49 Euro**)

Postage for shipping posters overseas by airmail:
+ 25 Euro

Postage for shipping posters within Europe by surface mail:
+ 15 Euro

Price list for reprints (The prices include mailing and handling charges. All Wiley-VCH prices are exclusive of VAT)

No. of pages	Price (in Euro) for orders of 50 copies	100 copies	150 copies	200 copies	300 copies	500 copies
1-4	345	395	425	445	548	752
5-8	490	573	608	636	784	1077
9-12	640	739	786	824	1016	1396
13-16	780	900	958	1004	1237	1701
17-20	930	1070	1138	1196	1489	2022
for every additional 4 pages	147	169	175	188	231	315

★ **Special Offer** ★ If you order 200 or more reprints you will get a PDF file for half price.

Wiley-VCH Verlag GmbH & Co. KGaA; Location of the Company: Weinheim;
Chairman of the Supervisory Board: Stephen Michael Smith,
Trade Register: Mannheim, HRB 432833, General Partner: John Wiley & Sons GmbH,
Location: Weinheim, Trade Register Mannheim, HRB 432296,
Managing Directors: Dr. Jon Walmsley, Sabine Steinbach

WILEY-VCH

WILEY-BLACKWELL

USING e-ANNOTATION TOOLS FOR ELECTRONIC PROOF CORRECTION

Required software to e-Annotate PDFs: Adobe Acrobat Professional or Adobe Reader (version 7.0 or above). (Note that this document uses screenshots from Adobe Reader X)
The latest version of Acrobat Reader can be downloaded for free at: http://get.adobe.com/uk/reader/

Once you have Acrobat Reader open on your computer, click on the Comment tab at the right of the toolbar:

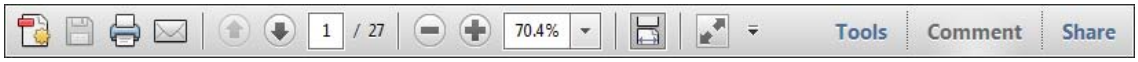

This will open up a panel down the right side of the document. The majority of tools you will use for annotating your proof will be in the Annotations section, pictured opposite. We've picked out some of these tools below:

1. Replace (Ins) Tool – for replacing text.

Strikes a line through text and opens up a text box where replacement text can be entered.

How to use it

- Highlight a word or sentence.
- Click on the Replace (Ins) icon in the Annotations section.
- Type the replacement text into the blue box that appears.

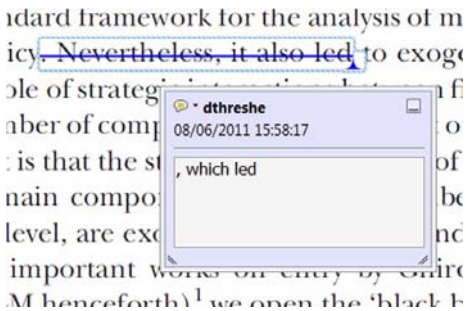

2. Strikethrough (Del) Tool – for deleting text.

Strikes a red line through text that is to be deleted.

How to use it

- Highlight a word or sentence.
- Click on the Strikethrough (Del) icon in the Annotations section.

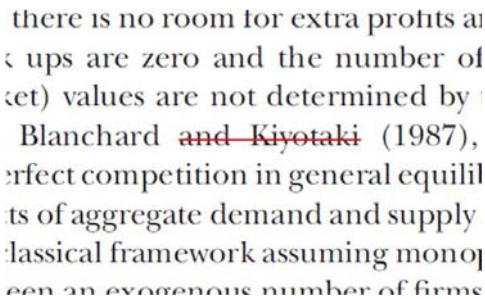

3. Add note to text Tool – for highlighting a section to be changed to bold or italic.

Highlights text in yellow and opens up a text box where comments can be entered.

How to use it

- Highlight the relevant section of text.
- Click on the Add note to text icon in the Annotations section.
- Type instruction on what should be changed regarding the text into the yellow box that appears.

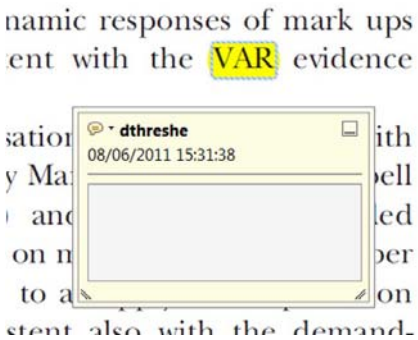

4. Add sticky note Tool – for making notes at specific points in the text.

Marks a point in the proof where a comment needs to be highlighted.

How to use it

- Click on the Add sticky note icon in the Annotations section.
- Click at the point in the proof where the comment should be inserted.
- Type the comment into the yellow box that appears.

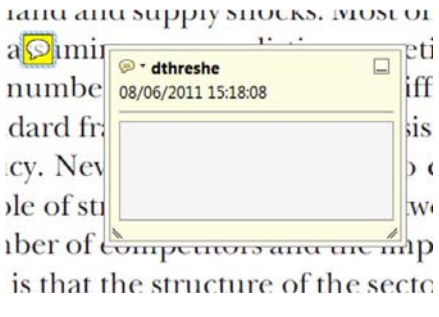

USING e-ANNOTATION TOOLS FOR ELECTRONIC PROOF CORRECTION

5. Attach File Tool – for inserting large amounts of text or replacement figures.

Inserts an icon linking to the attached file in the appropriate pace in the text.

How to use it

- Click on the Attach File icon in the Annotations section.
- Click on the proof to where you'd like the attached file to be linked.
- Select the file to be attached from your computer or network.
- Select the colour and type of icon that will appear in the proof. Click OK.

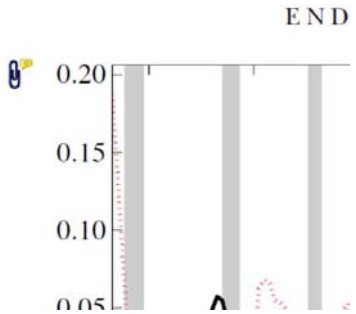

6. Add stamp Tool – for approving a proof if no corrections are required.

Inserts a selected stamp onto an appropriate place in the proof.

How to use it

- Click on the Add stamp icon in the Annotations section.
- Select the stamp you want to use. (The Approved stamp is usually available directly in the menu that appears).
- Click on the proof where you'd like the stamp to appear. (Where a proof is to be approved as it is, this would normally be on the first page).

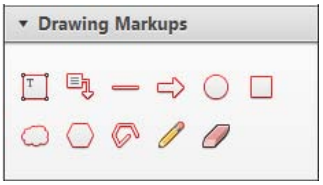

7. Drawing Markups Tools – for drawing shapes, lines and freeform annotations on proofs and commenting on these marks.

Allows shapes, lines and freeform annotations to be drawn on proofs and for comment to be made on these marks..

How to use it

- Click on one of the shapes in the Drawing Markups section.
- Click on the proof at the relevant point and draw the selected shape with the cursor.
- To add a comment to the drawn shape, move the cursor over the shape until an arrowhead appears.
- Double click on the shape and type any text in the red box that appears.

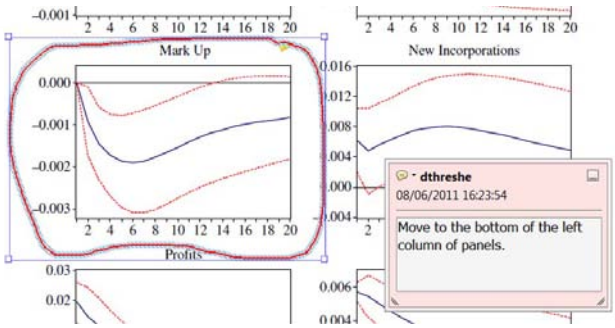

For further information on how to annotate proofs, click on the Help menu to reveal a list of further options: